Journal of Marine Research, 65, 789–812, 2007

Notes on the modeling of methane in aging hydrothermal plumes

by G. C. Nihous[1,2] and S. M. Masutani[1]

ABSTRACT

Marine hydrothermal vent fields represent a unique environment for the study of aerobic microbial methane oxidation because of high methane concentrations and limited spatial and temporal scales. Earlier data collected in lateral plumes at the Endeavour Segment of the Juan de Fuca Ridge, including methane concentration, methane oxidation rate and stable carbon isotopic composition ($\delta^{13}C$), are carefully interpreted with a suite of simple analytical models. Methane oxidation is defined with a rate constant k as a first order process with respect to both substrate and methanotroph concentration. This elementary formalism coupled with simplified representations of advection and diffusion through the lateral plume is sufficient to reproduce salient features of the data: maximum methane turnover times of about a week 2 km from the vent field location and stable carbon isotopic enrichment from -47‰ to values exceeding -5‰ over a distance of 15 km. Results suggest that k is of order 10^{-8} $(\text{nM-s})^{-1}$ at local conditions and that methane oxidizing bacteria hold about 12 fg of carbon per cell.

1. Introduction

In the first paragraphs of a recent comprehensive review of oceanic methane biogeochemistry, Reeburgh (2007) defined the challenge of better understanding the fate of methane in the ocean: the widespread nanomolar concentrations of this dissolved gas actually mask a competition of sorts between enormous seafloor additions and very efficient aerobic microbial oxidation. Yet, much remains to be learned about these processes.

Modeling a non-conservative species like methane in the ocean is fraught with difficulty since dispersal from turbulence and currents plays a major role alongside methane sources and sinks. The mediation of methane oxidation by bacterial assemblages (methanotrophs) of little-known characteristics also subject to dispersal and to their own sources and sinks represents a serious complication. Measurements of specific (first-order) methane oxidation rates from seawater samples are scarce and do not allow a differentiation between the possible effects of thermodynamic parameters (e.g temperature) and unknown concentra-

1. Hawaii Natural Energy Institute, School of Ocean and Earth Science and Technology, University of Hawaii, Honolulu, Hawaii, 96822, U.S.A.
2. Corresponding author. ***email: nihous@hawaii.edu***

tions of methanotrophs. Modeling studies and data suggest that for open-ocean conditions, instantaneous methane turnover times[3] of 40 to 70 years are typical (Rehder *et al.*, 1999; Valentine *et al.*, 2001; Nihous and Masutani, 2006). In coastal regions where significant seafloor input occurs, such as the Southern California Bight and Eel River Basin, turnover times are reduced to months (Ward and Kilpatrick, 1993; Valentine *et al*., 2001). In the close proximity of methane-rich hydrothermal vents, turnover times as short as a week have been reported (de Angelis *et al.*, 1993). This suggests that methanotroph concentrations vary widely in the oceans, and are far greater in areas of high substrate concentrations. The identification of marine aerobic methanotrophs and an understanding of their metabolism are therefore critical. These tasks are difficult and have been ongoing (Whittenbury *et al.*, 1970; Ward, 1987; Sieburth *et al.*, 1987,1993; Bowman *et al.*, 1997); some knowledge acquired from relatively easier lake studies may be useful as well (Harrits and Hanson, 1980; Jones *et al.*, 1984; Sundh *et al.*, 2005).

The goal of this study is to gain some insight into the most basic processes affecting the evolution of methane in the ocean. This will be done by considering a very special environment where (a) the space and time scales of dispersal are relatively small and may allow substantial simplifications of the flow field; (b) a large seafloor input of methane is sustained; and (c) much relevant experimental data have been collected. Some hydrothermal plumes generated by seafloor vents appear to have these favorable features. In particular, many measurements have been made in the vicinity of vent fields along the Endeavour Segment of the Juan de Fuca Ridge, at about 48N and 129W (Lupton *et al.*, 1985; de Angelis *et al.*, 1993; Johnson *et al.*, 2000; Cowen *et al.*, 2002).

In the next Section, basic physical characteristics of the buoyant plumes that rise from seafloor hydrothermal vents to a level of neutral buoyancy are briefly discussed. Biological and oxidation processes *per se* are not expected to play any role during the short ascent of these buoyant plumes, but some understanding of volume flux and dilution of the original vent fluids is useful to better characterize boundary conditions for the intrusion layer. The intrusion layer, or lateral far-field plume, slowly spreads over days at a nearly constant level above the seafloor and extends over several kilometers horizontally. In spite of considerable dilution of the vent fluid in the near-field, the far-field plume exhibits methane concentrations two orders of magnitude greater than in background seawater (de Angelis *et al.*, 1993; Cowen *et al.*, 2002). Such high initial substrate (methane) availability combined with relatively slow mixing dynamics provides ideal conditions for significant oxidation. This is evident in (a) the methane oxidation rates measured by de Angelis *et al.* (1993), described as "the highest such rates so far reported for the water column of any marine environment;" and (b) in the stable isotopic (^{13}C) composition data of Cowen *et al.* (2002), with $\delta^{13}C$ values "among the heaviest yet reported from a natural marine environment."

3. By convention, this is defined as the inverse of the specific methane oxidation rate, *Sp* i.e. the ratio of methane concentration over oxidation rate. It would be a true 'turnover time' only if the water mass remained unmixed.

Section 3 proposes simple far-field models of the evolution of methane concentration, isotopic composition and methanotroph-carbon concentration throughout the lateral plume. The goal of such models is to better parameterize aerobic oxidation by testing simple formalisms against data sets.

2. Near-field behavior of hydrothermal plumes

Simple arguments are presented here to characterize the behavior of the buoyant section of plumes generated in the vicinity of hydrothermal vents. The hydrodynamic near-field corresponds to the vertical rise of seafloor vent fluid and entrained seawater in a stratified environment until the mixture reaches neutral buoyancy; the distance h above the seafloor where vertical motion induced by buoyancy forces ceases is called the plume trap height. The more expansive lateral spreading of vertically stabilized plume fluid, or far-field, is analyzed in Section 3. We focus our attention on the example of the Endeavour Segment of the Juan de Fuca Ridge described in Lupton *et al.* (1985). The area of interest is a hydrothermal vent field of about 250 m by 150 m including about 40 active 'black smokers' at a water depth of about 2200 m.

Lupton *et al.* (1985) reported vent fluid dilutions of the order of 10^4 when the rising plume becomes neutrally buoyant about 200 m above the seafloor. This dilution magnitude was based on the ratio of estimated vent fluid temperature (300°C) over a measured temperature anomaly $\delta\theta \approx 0.05$°C in the lateral plume (far-field) 4.4 km away from the vent location. The authors' attempt to use plume theory, however, resulted in greater predicted dilutions (3.4×10^4) and a significantly higher neutral-buoyancy level h (370 m). Although the real fluid flow probably is complex and not sufficiently characterized, the lack of agreement with robust plume models warrants attention. Recent studies of hydrothermal plume behavior (Bemis *et al.*, 2002; Rona *et al.*, 2002) using acoustic imaging have generally validated classical plume theory (e.g. Morton *et al.*, 1956) as long the vents behaved like point sources of buoyancy and that multiple plumes remained sufficiently separated. Other issues that may be raised are the distance where the end-point temperature anomaly was measured and the fact that the entrainment of progressively warmer water in a vertically stratified environment complicates the determination of dilution from the end-point measurements of temperature anomaly. These ideas are succinctly explored below.

a. Buoyant plume without current

The thickness D of the laterally spreading plume (far-field) was estimated to be 180 m from CTD casts (Lupton *et al.*, 1985). The near equality $D \approx h$ between intrusion layer thickness and buoyant-plume trap height is characteristic of small currents U (Wright *et al.*, 1982; Roberts *et al.*, 1989). We consider here the case when U, perhaps in an average sense, is zero.

Several difficulties are encountered at this juncture. Point-source buoyant plumes entrain surrounding ambient fluid and widen as they rise; the plume radius b is predicted to grow linearly with height Z according to the equation $b = 1.2(6/5)EZ$ (Morton *et al.*, 1956). With b interpreted as an average value (top-hat profiles of plume parameters[4]), the entrainment coefficient E typically is 0.12. Considering 40 black smokers assumed to be spread uniformly in an area 250 m by 150 m (Lupton *et al.*, 1985), the plumes produced by individual smokers would merge at a height of 100 m above the seafloor, about half-way from reaching neutral buoyancy. Moreover, the lateral entrainment of ambient fluid in a rising plume closely surrounded by similar plumes is conceptually problematic since it would be inhibited by reason of symmetry; it is likely that this configuration might be best described as a distributed source of seafloor buoyancy drawing ambient fluid into a mixing boundary layer from which a plume(s) would buoyantly rise. Such a mechanism was experimentally and theoretically analyzed for the distributed injection of freshwater into brine (Epstein and Burelbach, 2001). Although the possible merging of individual plumes and their potential origin from a mixing layer would not permit a straightforward use of classical point-source plume theory, some insight may be gained by invoking this simpler framework as discussed below.

In stratified fluids, the buoyancy frequency $N = [(g/\rho_a)|d\rho_a/dZ|]^{1/2}$ is the theoretical frequency at which a vertically displaced fluid parcel would oscillate about its equilibrium position. When N is constant, Morton *et al.* (1956) derived the following estimate for h:

$$h = 3.79B(0)^{1/4}N^{-3/4} \tag{1}$$

g is the acceleration of gravity and Z the vertical coordinate measured from the seafloor; the ambient seawater density ρ_a, taken as $1000 + \sigma_2$ (potential density at a reference pressure of 2000 dbar) is calculated from Fofonoff and Millard (1983). B is the buoyancy flux defined as $Qg\delta\rho/\rho_{ref}$, where Q is the plume volume flux, $\delta\rho$ the density anomaly between plume and ambient fluids and ρ_{ref} a reference density. With $N^2 = 1.46 \times 10^{-6}$ s^{-2} (Lupton *et al.*, 1985) and $h \approx 200$ m, Eq. (1) implies an initial buoyancy flux of 0.0137 m^4/s^3, i.e. much less than the value of 0.17 m^4/s^3 cited by Lupton *et al.* (1985) for a single black smoker. Interestingly, the estimation of buoyancy fluxes from hot hydrothermal vents appears to be flawed (and skewed toward low values) in the technical literature (e.g. Bemis *et al.*, 2002). The buoyancy deficit term $\delta\rho/\rho_{ref}$ usually is obtained by multiplying the temperature difference between seawater and vent fluids, $\theta_0 - \theta_a(0)$, by the local thermal expansion coefficient for seawater $a \approx 1.5 \times 10^{-4}$°C^{-1}. With $\theta_0 - \theta_a(0)$ of the order of 300°C, however, the linearity of water density with temperature breaks down as shown in Figure 1 (freshwater data at a constant pressure of 20.101325 MPa from NIST, 2005); the substantial variation of density over the temperature range of interest also suggests that the

4. In the original derivation of plume theory, plume characteristics are assumed to have transverse Gaussian profiles; the conservation equations can be recast by assuming top-hat profiles instead, i.e., constant transverse characteristics; with Gaussian profiles, b is the e-folding radius and E is $\sqrt{2}$ smaller.

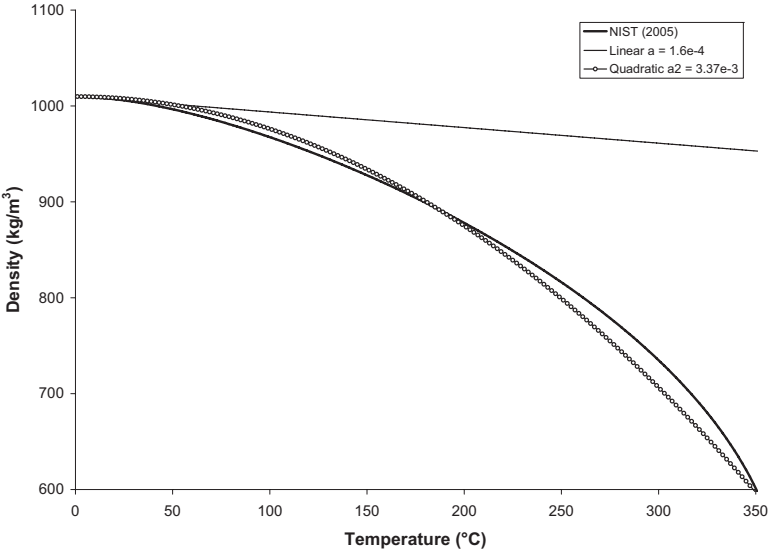

Figure 1. Density of fresh water at constant pressure (20.101325 MPa).

Boussinesq approximation, whereby fluid density is assumed constant except in defining weight and buoyancy forces, may not be acceptable for fluid models as in Epstein and Burelbach (2001). Our estimate of $B(0)$ corresponds to a buoyant rise time of about half an hour deemed typical of hydrothermal vent environments (Rona *et al.*, 2002).

We define the reference density as $\rho_{ref} = \rho_a(0) = 1000 + \sigma_2(1.80°C, 34.6\ ppt) = 1036.9$ kg/m^3. Ambient and vent fluids appear to have similar salinities s at the release point (Lupton *et al.*, 1985). The density ρ_0 of 300°C hydrothermal vent fluid is estimated to be 756.9 kg/m^3 by applying a salinity correction of 0.64 s (Epstein and Burelbach, 2001) to the freshwater data. With our estimate of $B(0)$, this would correspond to $Q(0) = 5.17 \times 10^{-3}$ m^3/s. Note that $Q(0)$ usually is assessed from field observation. Formulas for the volume flux of buoyant plumes in unstratified fluids are for the most part applicable in slightly stratified environments (Nihous, 2006). For top-hat profiles in the absence of currents, the following equation can be used (Wright, 1977; Huang *et al.*, 1998):

$$Q = 0.2B(0)^{1/3}Z^{5/3}. \tag{2}$$

With $Q(h) = 327$ m^3/s, the dilution $Q(h)/Q(0)$ would be of the order of 6.3×10^4. Thus, a derivation where h constrains $B(0)$ via Eq. (1) and where the hydrothermal vent fluid temperature θ_0 defines the initial density deficit yields much greater dilution than was observed.

An alternative approach is to consider $\theta(0)$ to be unknown as long as the heat input from a typical single black smoker $H(0) \approx Q(0)\rho(0)c_p(0)\theta(0)$ is given (e.g. 10^7 cal/s in Lupton *et al.*, 1985). Both density ρ and specific enthalpy c_p depend on temperature. If $B(0)$ also is available, an implicit equation in $\theta(0)$ can be obtained by eliminating $Q(0)$:

$$\theta(0)c_p(0)\left\{\frac{\rho_{ref}}{\rho(0)}-1\right\}^{-1}=\frac{gH(0)}{B(0)\rho_{ref}}. \tag{3}$$

The right-hand side being known, a solution of Eq. (3) yields $\theta(0) \approx 11°C$. Such a low value could suggest the existence of a seafloor mixing layer formed by a distributed vent source where a dilution of the vent fluid of the order of 30 would take place. This idea is explored in some details in the Appendix. It can be shown that a circular source about 1.4 m in diameter releasing 300°C hot vent fluid at 2 cm/s would yield such a value of $\theta(0)$ less than a meter above the seafloor. Visual observations of vents typically yield high release velocities ($\sim$ 1 m/s) over small areas (effective diameter $\sim$ 3 cm) instead (Rona *et al.*, 2002). While simple models and scant observations are not likely to offer definitive answers, the mixing-layer paradigm may support the notion expressed in Lupton *et al.* (1985) that "although black smokers are the most visible type of discharge. . .a large fraction of the [plume] effluent layer may be the result of diffuse hydrothermal flows. . ."

From solving Eq. (3), we also find that $Q(0) = 0.92$ m^3/s so that within the rising plume, an additional dilution of 355 takes place. This corresponds to an overall volume dilution of 1.1 x 10^4 in much better agreement with observations. With the product $\rho\ c_p$ nearly constant at 4.14 x 10^6 J-m^{-3}-K^{-1} and using Eq. (2), the 'temperature flux' $Q\theta$ satisfies the following approximate equation:

$$\frac{d(Q\theta)}{dZ}=\frac{1}{3}B(0)^{1/3}Z^{2/3}\theta_a(Z). \tag{4}$$

Linearizing the ambient temperature profile as $\theta_a(Z) = 1.8 + 6.5 \text{ x } 10^{-4}Z$ (Lupton *et al.*, 1985) makes the integration of Eq. (4) between 0 and h straightforward. As the plume reaches neutral buoyancy, the temperature anomaly $\delta\theta = \theta_a(h) - \theta(h)$ can be derived from the solution. Unfortunately, the initial value $Q(0)\theta(0)$ obtained by solving Eq. (3) with $H(0) = 10^7$ cal/s is too small to yield a positive temperature anomaly at $Z = h$. It can be shown that a necessary condition for $\delta\theta > 0$ is $Q(0)\theta(0) > 15.3$ m^3-K-s^{-1}. With greater hydrothermal heat input, estimates of overall dilution and temperature anomaly could be consistent with observations. $H(0) = 4 \times 10^7$ cal/s, for example, corresponds to an overall dilution of 9000, $\delta\theta = 0.0763°C$, $\theta(0) = 2.5°C$ and $Q(0) = 16.1$ m^3/s; the near-ambient value of $\theta(0)$ would suggest intense mixing near the seafloor, however.

b. Buoyant plume in current

de Angelis *et al.* (1993) reported typical horizontal currents of the order of 1 km per day in the area of interest. This value of U is rather small but could alter the dynamics of the buoyant hydrothermal plumes. Here, we simply retrace the steps of the simple analysis presented when $U = 0$. An equivalent of Eq. (1) is given by Hewett *et al.* (1971)

$$h = 1.7B(0)^{1/3}U^{-1/3}N^{-2/3}. \tag{5}$$

With $h = 200$ m, the initial buoyancy flux $B(0)$ would be 0.0275 m^4/s^3. This would correspond to $Q(h) = 413.5$ m^3/s from Huang *et al.* (1998). Assuming the plume to originate from a 300°C point source results in excessive dilution, of the order of 4×10^4, as before. Solving Eq. (3) instead yields $\theta(0) \approx 43$°C and $Q(0) = 0.24$ m^3/s, for an overall volume dilution of 1.2×10^4. With such values, the mixing-layer model would correspond to a distributed source only about half a meter in diameter with an average release velocity of about 0.2 m/s. Finally, repeating the estimation of the temperature anomaly at neutral buoyancy by integrating Eq. (4), we find that $\delta\theta < 0$ unless higher values of $H(0)$ are allowed.

3. Far-field models of methane in hydrothermal plumes

To gain some insight into aerobic methane oxidation processes, a suite of simple steady-state models describing the neutrally-buoyant phase (far-field) of the plumes generated by hydrothermal vents is presented. Three variables of interest are methane concentration x, carbon-13 methane ($^{13}CH_4$) concentration y and methanotroph carbon concentration z. The isotopic composition of methane is given by $\delta^{13}C(‰) = 1000\{y/\{R_{PDB}(x - y)\} - 1\}$, where R_{PDB} is the isotopic ratio of the PDB standard equal to 0.011237 (Craig, 1957). The steady-state equations for x, y and z can be written:

$$\begin{cases} (\vec{u} \cdot \nabla)x - \nabla \cdot (K\nabla x) = -kxz & \text{(6.a)} \\ (\vec{u} \cdot \nabla)y - \nabla \cdot (K\nabla y) = -\dfrac{kxyz}{y + \alpha_k(x - y)} & \text{(6.b)} \\ (\vec{u} \cdot \nabla)z - \nabla \cdot (K\nabla z) = \alpha kxz. & \text{(6.c)} \end{cases}$$

Since vertical transport phenomena are considered negligible through the laterally spreading plumes, the equations are two-dimensional in a horizontal fluid domain of uniform thickness. Accordingly, the velocity vector $\vec{u}$ and eddy diffusion coefficient K are defined in a horizontal plane (X, Y), and the Nabla operator reduces to $\nabla = (\partial/\partial X, \partial/\partial Y)$. The right-hand sides of Eq. (6) reflect the non-conservative behavior of methane-related species. In Eq. (6.a), methane oxidation is assumed to be proportional to x and z with a basic rate constant k. This formulation implies that methane concentrations are well below kinetic saturation levels; a study of methanotroph communities in Lake Mendota (Harrits and Hanson, 1980) suggests a half-saturation constant of the order of 1 to 5 μM, while experiments conducted by Ward (1987) on *Nitrosococcus oceanus* yielded a value of 6.6 μM. At the same time, methane concentrations in the plumes under consideration are much higher than possible low oxidation thresholds of the order of 1 nM that may inhibit methanotroph growth (Scranton and Brewer, 1978; Nihous and Masutani, 2006). Eq. (6.b) reflects the preferential uptake of $^{12}CH_4$ during oxidation and subsequent $^{13}CH_4$ enrichment of the ambient water; the apparently complicated form of the right-hand side stems from the definition of the fractionation factor α_k; with α_k slightly larger than one and $x \gg y$, the sink of $^{13}CH_4$ can be closely approximated by $-kyz/\alpha_k$. Eq. (6.c) assumes that methane

is a limiting substrate for methanotroph growth with an assimilation ratio α, although other nutrients like ammonium are consumed (Jones *et al.*, 1984; Ward, 1987; Cowen *et al.*, 2002). Over characteristic time scales for plume spreading, it is also assumed for lack of better knowledge that any sink balancing methanotroph growth is negligible. In plankton community models, for example, closure of the equations to better fit observations is achieved by incorporating a mortality term proportional to the square of plankton concentration (Steele and Henderson, 1992); such model refinements obviously rest on the availability of sufficient data.

a. A closed-form solution in the absence of diffusion

If diffusion is ignored ($K = 0$), the differential Eq. (6) are first-order only. With a uniform current field of magnitude U flowing along a prescribed direction X, the advective operator in the left-hand sides simply is $U\mathrm{d}/\mathrm{d}X$. The resulting system of equations yields closed form solutions when the sink of $^{13}CH_4$ is approximated by $-kyz/\alpha_k$. Algebraic manipulations are not detailed here since they present no particular difficulty with standard tables of indefinite integrals (e.g. Weast, 1975). Assigning the subscript 0 to quantities at the origin of the lateral plume $X = 0$, we obtain:

$$\begin{cases} x = \dfrac{\left(\dfrac{\alpha x_0^2}{z_0} + x_0\right)\exp\left\{-(\alpha x_0 + z_0)\dfrac{kX}{U}\right\}}{1 + \dfrac{\alpha x_0}{z_0}\exp\left\{-(\alpha x_0 + z_0)\dfrac{kX}{U}\right\}} & (7.a) \\ y = \dfrac{y_0\left(1 + \dfrac{\alpha x_0}{z_0}\right)^{1/\alpha_k}\exp\left\{-(\alpha x_0 + z_0)\dfrac{kX}{\alpha_k U}\right\}}{\left[1 + \dfrac{\alpha x_0}{z_0}\exp\left\{-(\alpha x_0 + z_0)\dfrac{kX}{U}\right\}\right]^{1/\alpha_k}} & (7.b) \\ z = \dfrac{\alpha x_0 + z_0}{1 + \dfrac{\alpha x_0}{z_0}\exp\left\{-(\alpha x_0 + z_0)\dfrac{kX}{U}\right\}}. & (7.c) \end{cases}$$

It is clear even before integration that the identity $\alpha x + z = \alpha x_0 + z_0$ holds everywhere. In particular, methane is consumed completely and methanotroph carbon concentration reaches the asymptotic value $\alpha x_0 + z_0$ as downstream distance X tends to infinity. With diffusion, however, z would be expected to reach a maximum instead. This is confirmed by measurements of specific methane oxidation rates $Sp = kz$ and bacterial cell counts as a function of X performed in lateral plumes of the Endeavour Segment (Fig. 6 and 8 in de Angelis *et al.*, 1993); the maxima are reached within 4 km downstream of the vent locations and typically represent a two- to four-fold increase over initial values. If methane oxidation proceeds rapidly enough in the neighborhood of the hydrothermal vents, a measured peak in specific oxidation rate could be interpreted as the asymptotic value of the

zero-diffusion model. The knowledge of α, x_0 and the maximum of $Sp/Sp_0 = z/z_0$ would then yield estimates of z_0. With $\alpha \approx 0.30$ (de Angelis *et al.*, 1993) to 0.50 (Ward, 1987) and $x_0 \approx 400$ (de Angelis *et al.*, 1993) to 600 nM (Cowen *et al.*, 2002), values of Sp/Sp_0 between two and four imply that $z_0 \approx 100$ nM.

In turn, the rate constant k can be constrained by the ratio Sp_0/z_0. With measured specific oxidation rates of 0.02 to 0.08 day^{-1} at the origin of the lateral plume $X \approx 0$ (de Angelis *et al.*, 1993), we infer that k must be of order 10^{-9} to 10^{-8} nM^{-1}-s^{-1}. In a study of aerobic methane oxidation in three small temperate lakes, Sundh *et al.* (2005) recently published methanotroph biomass-specific oxidation rates $Spm = kx$. Of particular interest is their Figure 5a which shows Spm as a function of methane concentration x; for methane concentrations between 100 and 500 nM, the cluster of data for Spm (0.025 to 0.2 day^{-1}) would correspond to the rate constant k ranging from 10^{-9} to 1.7 x 10^{-8} nM^{-1}-s^{-1}. The agreement with our estimate is remarkably close and it would be tempting to conclude that similarities in both environments (e.g. cold) may be more significant than differences (e.g. salinity, pressure). Since different methanotrophs are likely to be involved, however, some caution must be exercised. De Angelis *et al.* (1991) showed that for a given deep-water microbial assemblage, hydrostatic pressure favored methane oxidizing activity. While Sieburth *et al.* (1987) discovered that *Methylomonas pelagica* can grow over a wide range of salinities (4 to 32 ppt), other marine methanotrophs such as *Methylosphaera hansonii* require seawater to thrive (Bowman *et al.*, 1997). Therefore, the above estimates of k may only suggest that the order of magnitude of the methane oxidation constant seems to be the same for methanotrophs adapted to the salinity and pressure of their natural environment.

The rise in measured bacterial cell counts, from about 7 x 10^5 ml^{-1} to 9 x 10^5 ml^{-1} (Fig. 8 in de Angelis *et al.*, 1993) does not match that in specific oxidation rates, although Sp is by definition proportional to z. A simple explanation is that only a fraction of the bacterial population represents methanotrophs; the data under consideration would suggest that the methanotroph count is of the order of 10^5 ml^{-1} at $X \approx 0$. This corresponds to the proportion of methanotrophs approximately increasing from 1/7 to 1/3 in the initial spreading stage of the lateral plume. Such values are somewhat smaller than methanotroph biomass fractions as high as 41% reported by Sundh *et al.* (2005); this may be expected since hydrothermal plumes in the deep ocean represent a more open and dynamically changing environment than small stratified lakes.

Dividing $z_0 \approx 100$ nM-C by the estimated cell count at $X \approx 0$ yields a methanotroph carbon content of 12 fg-C/cell. This coincides with the measured value published by Fukuda *et al.* (1998) for marine bacterial assemblages separated through a 0.8 μm filter. Other estimates such as 20 fg-C/cell (DeLong, 1999) or 10 to 50 fg-dry-weight/cell (Button and Robertson, 1999) are close since, for the latter reference, carbon contents typically represents 50% of bacterial dry weight (Sundh *et al.*, 2005). The summertime data of Sundh *et al.* (2005) collected at about 8 m depth in Illersjön Lake were carefully examined since they correspond to a methanotroph proportion of about 40% (ratio of the characteristic methanotroph phospholipid fatty acid 16:1ω8c concentration over the common bacte-

rial phospholipid fatty acid 18:1ω7c concentration, Fig. 3d). We could estimate the methanotroph carbon content to be 11 fg-C/cell, from a methanotroph biomass of about 15 ng-C-ml^{-1} (30 ng-dry-weight-ml^{-1}, Fig. 4) and a methanotroph cell count of 1.36 x 10^{6} ml^{-1} (0.4 times 3.4 x 10^{6} ml^{-1}, Fig. 1 or 2b).

Sundh *et al.* (2005) noted that their values of *Spm* are much smaller than published data from laboratory cultures of methanotrophs in the range 2.0 x 10^{-5} to 2.4 x 10^{-4} s^{-1} (50 to 600 nmol per mg-dry-weight per min). An example of high biomass-specific oxidation rate can be found in Ward (1987), at 2.2 x 10^{-10} μmol per cell per hour; with 12 fg-C per cell, this translates to 6.1 x 10^{-5} s^{-1}; with a methane substrate concentration of 75 nM, the value of k corresponding to her incubation experiments would be as high as 8 x 10^{-7} nM^{-1}-s^{-1}, i.e. two orders of magnitude higher than our estimate. One possible factor is temperature since the far- field of deep marine hydrothermal plumes as well as the hypolimnion of high-latitude lakes is cold, while laboratory cultures typically are conducted at 'room temperature'. As a matter of fact, Sieburth *et al.* (1987) concluded that *Methylomonas pelagica* did not grow at 10°C (or below). Harrits and Hanson (1980) showed that between 4°C and 22°C, methane oxidation rates increased by a factor of nine for lake methanotrophs, all other things being equal. In an early study of aerobic oxidation mediated by bacteria from marine sediments, Hutton and Zobell (1949) reported that one incubation experiment at low temperature (3°C to 5°C) took 9 months before producing conclusive results, instead of a few days at room temperature.

Eq. (7) were considered with $\alpha = 0.30$ (de Angelis *et al.*, 1993), and the following parameters from Cowen *et al.* (2002): $x_0 = 600$ nM, $y_0 = 6.357$ nM (or $\delta^{13}C = -47‰$ at the origin), $\alpha_k = 1.0075$ and a target value $\delta^{13}C = -5‰$ at a distance $X = 15$ km. The isotopic fractionation factor is very close to the mean value (1.008) derived by Grant and Whiticar (2002) near cold seeps above Hydrate Ridge, Cascadia Oregon Margin; since Cowen *et al.* (2002) were able to correct for potential mixing effects by using temperature anomaly, it is probable that mixing did not significantly affect the results of Grant and Whiticar (2002). z_0 was varied upward from 50 nM to 260 nM. For this initial methanotroph carbon concentrations and with $U = 1$ km/day, the target isotopic enrichment is reached for k between 2.4 x 10^{-8} and 1.1 x 10^{-8} nM^{-1}-s^{-1}. The solution is invariant if k and U remain proportional so that a current of 500 m/day would correspond to k between 1.2 x 10^{-8} and 6.1 x 10^{-9} nM^{-1}-s^{-1}. Our earlier inference that k should be of order 10^{-9} to 10^{-8} nM^{-1}-s^{-1} was not reached using any ^{13}C isotopic measurement. Yet, this range of methane oxidation rate constants successfully reproduces measured $\delta^{13}C$ values, 15 km away from the vent location, that are "among the heaviest yet reported from a natural marine environment" (Cowen *et al.*, 2002).

b. An axisymmetric model without current

Many black smokers ($n \approx 40$) potentially representative of 'point sources' were identified in the area under consideration (Lupton *et al.*, 1985). With the estimate $Q(h) =$ 327 m^3/s made in Section 2a for each individual buoyant plume, an overall volume flux Q_f

of about 1.3 x 10^4 m^3/s would feed the lateral (far-field) plume of thickness $D = 180$ m. With negligible currents, at least in an average sense, the lateral plume would be axisymmetric and the far-field Eq. (6) one-dimensional in the radial direction r. Assuming a horizontal eddy diffusivity $K = Pr$ based on the concept of diffusion velocity (Joseph and Sendner, 1958), the advection-diffusion operator in Eq. (6) can be written $\frac{Q_f}{2\pi Dr}\frac{\partial}{\partial r} - \frac{1}{r}\frac{\partial}{\partial r}\left(Pr^2\frac{\partial}{\partial r}\right)$; the choice of the advection term corresponds to a zero initial radius with an integrable velocity singularity (Nihous, 2007). For any conservative species such as the temperature anomaly $\delta\theta$, the steady-state equation would consist in setting this operator to zero; the solution is:

$$\delta\theta = \delta\theta|_{r=0}\left\{1 - \exp\left(-\frac{Q_f}{2\pi DPr}\right)\right\}. \tag{8}$$

This also is the recommended formula to estimate the concentration of discharged pollutants in the ocean found in the Screening Information Data Set (SIDS) of the United Nations Environmental Program (2000). With $P \sim 1$ mm/s and the values of Q_f and D above, the temperature anomaly would be halved approximately 15 km away from the vent location. This corresponds to a characteristic length $r_f = Q_f/(2\pi DP)$ of about 12 km. Temperature-anomaly data from Cowen *et al.* (2002), e.g. in their Figure 5A, are not easy to interpret; in particular, there seems to be an outlier ($\delta\theta \approx 0.12$) for the location farthest from the vent location (Station 10, 15 km away). If this point is excluded, data at Station 10 suggest a characteristic length of about 16 km; if the next most remote sampling location (Station 2, 3 km away) is used instead, r_f would be about 3 km. Although it may not represent a reliable parametric constraint, a value r_f of the order of 10 km is anticipated.

Eq. (6) for methane-related species and the proposed axisymmetric configuration were solved next in a region extending 60 km radially from the vent location. The same values of α, x_0, and y_0 as in Section 3a were selected, as well as a slightly larger isotopic fractionation constant $\alpha_k = 1.0077$, still consistent with Cowen *et al.* (2002), and a baseline value z_0 equal to 100 nM. With a numerical domain considerably larger than the sampled area, Dirichlet conditions were applied at the outside boundary, namely a methane concentration of 2 nM, a ^{13}C-methane concentration based on $\delta^{13}C = -43‰$ and a methanotroph carbon concentration corresponding to a background turnover time of 50 years (Rehder *et al.*, 1999; Valentine *et al.*, 2001; Nihous and Masutani, 2006). k, P and Q_f were varied in order to match the following experimental targets as well as possible: the mean values of $\delta^{13}C$ measured by Cowen *et al.* (2002) at several sampling stations, and the specific methane oxidation rates reported by de Angelis *et al.* (1993); these data are proxies for the variables y and z, respectively. The use of data collected nearly a decade apart to validate a specific model run is only justifiable if the hydrothermal vent system under consideration is stable over at least the same period. The characteristics of hydrothermal vent emissions along the Endeavour Segment of the Juan de Fuca Ridge were altered following moderate tectonic events in 1999 (Johnson *et al.*, 2000). Although the permanence of such changes is

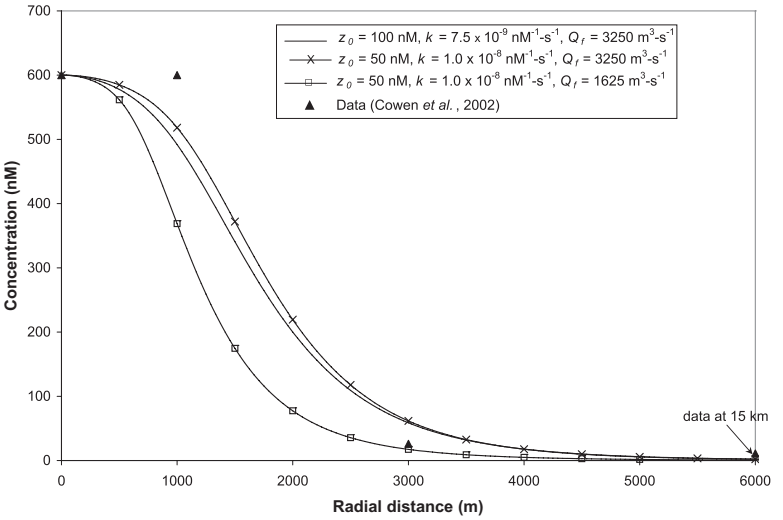

Figure 2. Predicted methane concentration (axisymmetric model).

unknown, flow rates were estimated to have increased in the couple of months following the earthquakes, while data were logged. It will be seen that model predictions are consistent with Q_f increasing between the times at which the data of de Angelis *et al.* (1993) and that of Cowen *et al.* (2002) were collected.

The parameters k, P and Q_f were swept to identify trends, and manually tuned thereafter. This task was somewhat simplified by the fact that predictions of the isotopic composition and of the specific oxidation rates often responded in opposite ways as a single parameter changed. Parametric variations where r_f or Sp_0 are constrained were also examined; in the latter case, a change in k was adjusted with a different value of z_0. A combination that yielded results that fit the data reasonably well is $k = 7.5 \times 10^{-9}$ nM^{-1}-s^{-1}, $P = 3 \times 10^{-4}$ m/s and $Q_f = 3250$ m^3/s; this volume flux is only a quarter of the estimate based on 40 black smokers and the analysis from Section 2a; it corresponds to $r_f \approx 10$ km. A variation where k increases to 1.0 x 10^{-8} nM^{-1}-s^{-1} while z_0 drops to 50 nM was considered as well. Finally, a third combination with $k = 1.0 \times 10^{-8}$ nM^{-1}-s^{-1}, $z_0 = 50$ nM and $Q_f = 1625$ m^3/s was selected. All values of k and z_0 are consistent with the estimates derived in Section 3a.

Predicted methane concentrations shown in Figure 2 rapidly drop with distance. This decline is representative of active microbial oxidation. Calculations agree reasonably well with observations given the steepness of the curve and the risk of sampling away from the plume core (17 - 62 nM at $r \sim 3$ km versus 26 nM in Cowen *et al.*, 2002). At greater distances, however, calculated values fall well below observed residual concentrations (0.01 nM at $r \sim 15$ km versus < 5.4 nM in de Angelis *et al.* (1993) and < 11 nM in Cowen *et al.* (2002)). Figure 3 displays predictions of isotopic compositions. The data of Cowen *et al.* (2002) are well reproduced with the two parametric combinations corresponding to the larger flow ($Q_f = 3250$ m^3/s); in those cases, the very strong ^{13}C enrichment about 15 km

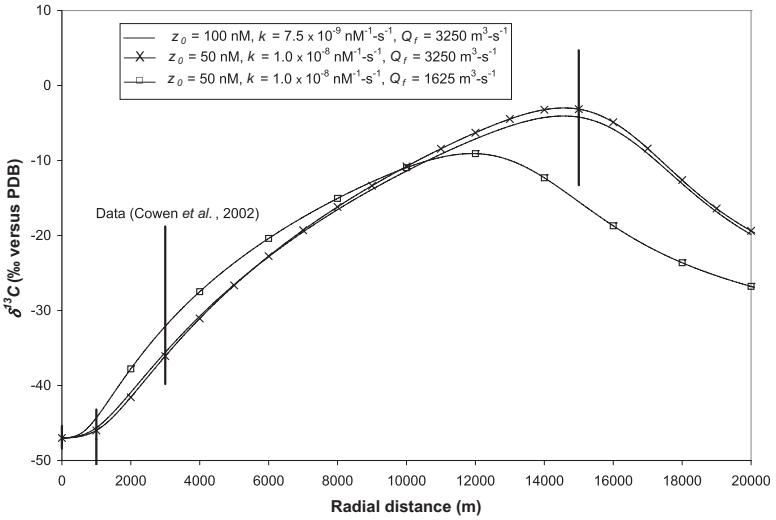

Figure 3. Predicted isotopic composition (axisymmetric model) and data of Cowen *et al.* (2002) shown as vertical bars.

away from the vent location is predicted as a maximum, although no data collected at greater distances can ascertain that the maximum does not occur further. With the smaller flow, enrichment does not reach high enough levels at great enough distances. Finally, the specific oxidation rates measured by de Angelis *et al.* (2003) were compared to model calculations as shown in Figure 4. Here, the lower flow ($Q_f = 1625$ m^3/s) yields oxidation rates that closely represent the upper envelope of the data set; in contrast, the higher flow leads to overestimated oxidation rates at radial distances beyond about 3 km. This suggests that flow rates may have been lower in 1991 than in 2000. In all cases, maximum oxidation rates occur about 2 to 3 km away from the vent location; such distance corresponds to the time lag during which methanotroph growth outweighs dispersal. $\delta^{13}C$ is defined with a ratio of isotopic species that both undergo dispersal so that the effect of the oxidation process on ^{13}C enrichment extends much further; this is clearly demonstrated by experimental and model results.

c. A two-dimensional model with current

Here, the simple analysis performed in Section 3a for a uniform current U is extended when horizontal eddy diffusivity is included ($K \neq 0$). The diffusive term in Eq. (6) involves two horizontal dimensions X and Y. Numerical solutions were obtained with a commercial finite-element solver (FEMLAB® 3, Version 3.1, COMSOL, Inc., 2003). For a continuous source in a current field, the parameterization of K with a diffusion velocity, as in Section 3b, is not justified *a priori*: with $U \neq 0$, the size of expanding and drifting 'patches' cannot be defined unambiguously by a distance like r referred to a unique center. K was taken constant instead (Fickian diffusion). Although this model is spatially more complex than

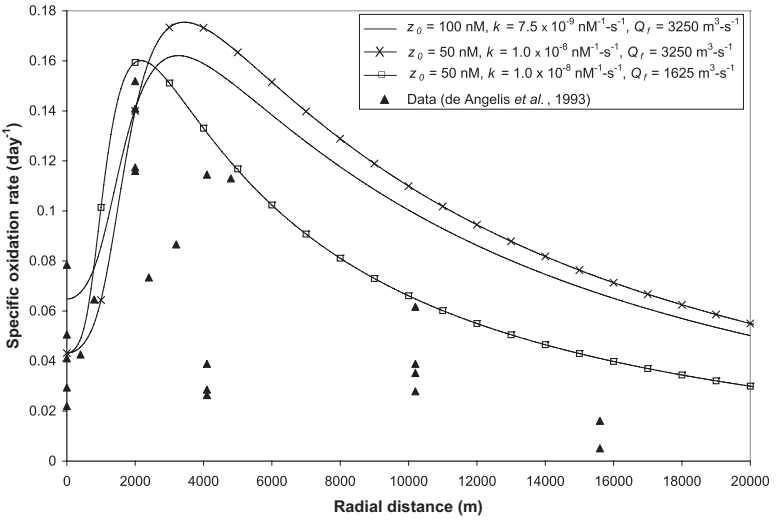

Figure 4. Predicted specific methane oxidation rate (axisymmetric model) and data of de Angelis *et al.* (1993).

the axisymmetric one, the very simple representations of the current field and of turbulent diffusion may offset any potential gain in predictive capabilities. The numerical domain was represented by a square 60 km by 60 km of implicit thickness D. Ambient concentrations were enforced on all boundaries except for a line of width $Q_f/(DU)$ at $X = 0$, corresponding to the transition from near-field to far-field, and for the downstream open boundary where convective fluxes (zero gradient) were chosen.

Numerical simulations showed that matching the target oxidation rate and isotopic composition data simultaneously would be difficult with constant advection. Results in relatively good agreement with data were obtained with $k = 1.0 \times 10^{-8}$ nM^{-1}-s^{-1}, $z_0 = 50$ nM, $K = 1$ m^2-s^{-1} and $U = 250$ m-day^{-1}, as shown in Figures 5 and 6. The width of the near-field-to-far-field transition line was about 8 km as Q_f was taken to be 10 times the value of $Q(h)$ estimated in Section 2b. The full solutions for the temperature anomaly, methane concentration, isotopic composition and specific methane oxidation rate are shown in Figures 7 through 10. Figure 11 displays selected half sections of calculated values of $\delta^{13}C$ in the cross-current direction; it can be seen that a 2 km off-axis measurement would underestimate the 'true' peak by about 4‰ at $X = 10$ km, 8‰ at $X = 15$ km, and 11‰ for X between 15 and 30 km.

4. Conclusions

This study presented simple models of ^{12}C-methane, ^{13}C-methane and methanotroph-carbon concentrations in neutrally-buoyant plumes generated in the vicinity of hydrothermal seafloor vent fields. Such specific marine environments provide unique opportunities

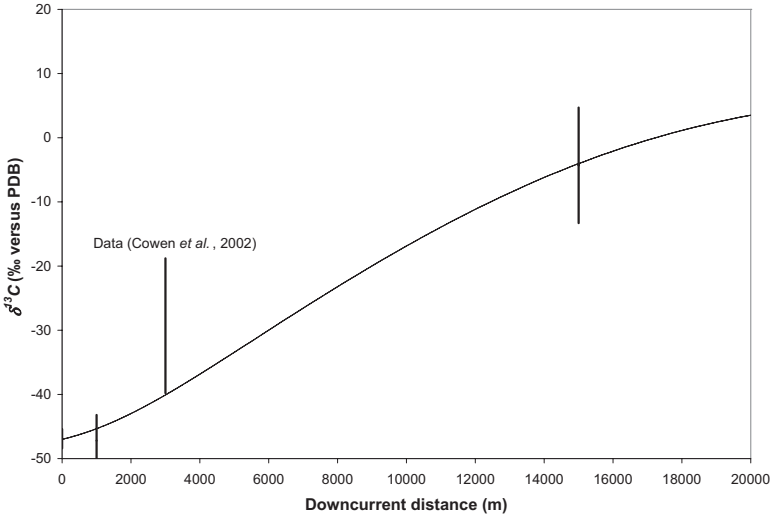

Figure 5. Predicted isotopic composition (two-dimensional model, solid line) and data of Cowen *et al.* (2002) shown as vertical bars.

to improve our understanding of aerobic methane oxidation mediated by bacterial assemblages because methane concentrations are a couple of orders of magnitude greater than in typical 'background' waters, while the spatial and temporal scales of the plume are sufficiently small to account for dispersal (from advection and diffusion) in relatively

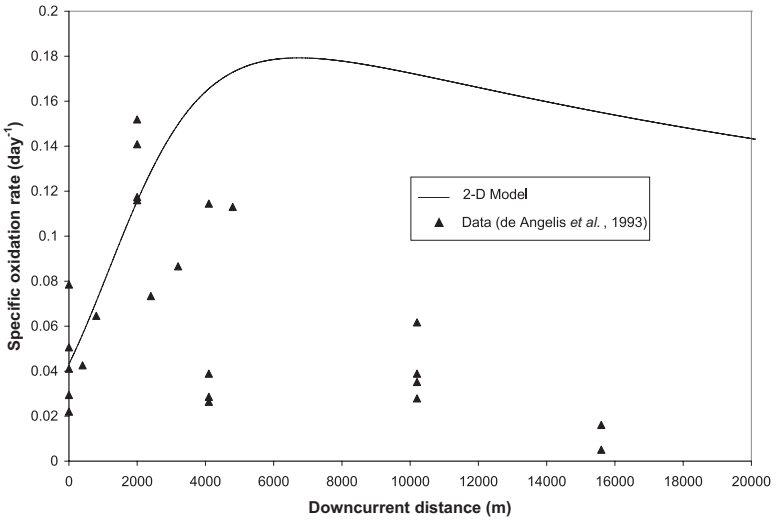

Figure 6. Predicted specific methane oxidation rate (two-dimensional model) and data of de Angelis *et al.* (1993).

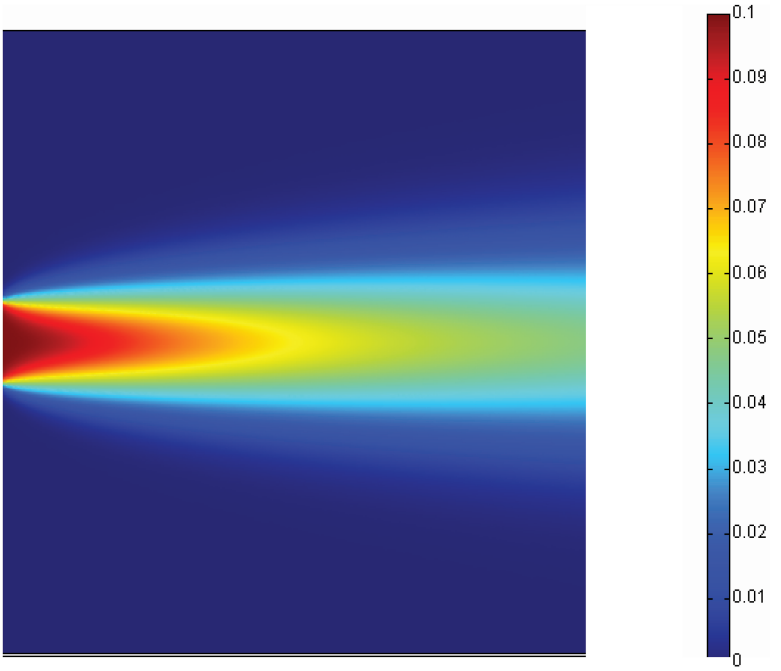

Figure 7. Predicted temperature anomaly in a horizontal domain 60 km by 60 km (°C).

simple ways. Data collected in lateral plumes at the Endeavour Segment of the Juan de Fuca Ridge were used to provide boundary conditions, a few key parameters (e.g. isotopic fractionation) and, more importantly, validation targets for the models. As a preliminary step to constrain volume flux, observed features of the buoyant plumes (near-field) such as trap height and dilution were reviewed using elementary plume theory; using an average heat input from the vents rather than hydrothermal fluid temperature suggested that vents may not behave like simple point sources and that a consistent representation of the near-field has yet to be achieved. Methane oxidation was defined with a rate constant k as a first order process with respect to both substrate and methanotroph concentration. This elementary formalism, imbedded in model source and sink terms, proved sufficient to reproduce salient features of the data: maximum methane turnover times of about a week 2 km from the vent field location and stable carbon isotopic enrichment from -47‰ to values exceeding -5‰ over a distance of 15 km. The modeling process suggested that k is of order 10^{-8} (nM-s)$^{-1}$ at local conditions and that the carbon content of methane oxidizing bacteria is about 12 fg (12 x 10^{-15} g) per cell. The rate constant appears to be much smaller than those inferred from laboratory incubation experiments (e.g. Ward, 1987); large apparent discrepancies between *in situ* and laboratory oxidation kinetic parameters were also reported in a recent temperate-lake study (Sundh *et al.*, 2005); temperature could be an important factor affecting k. 'Initial' methanotroph carbon concentrations of about 50 to100 nM above the vent field were inferred as well; this amount allowed predicted

Figure 8. Predicted methane concentration in a horizontal domain 60 km by 60 km (nM).

values to sharply increase within a couple of kilometers as demonstrated by oxidation rate data (de Angelis *et al.*, 1993); at its peak, the methanotroph population would represent about a third of the measured overall bacterial cell count. Finally, the tuning

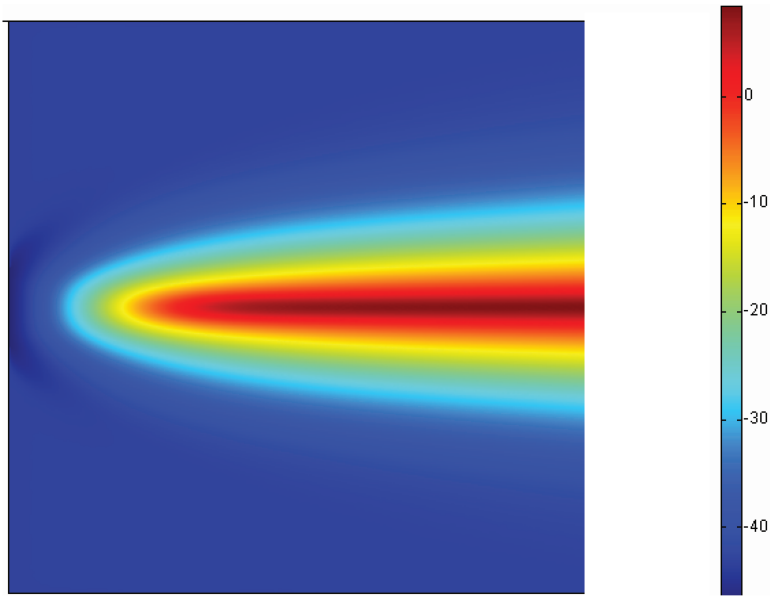

Figure 9. Predicted isotopic composition in a horizontal domain 60 km by 60 km (‰).

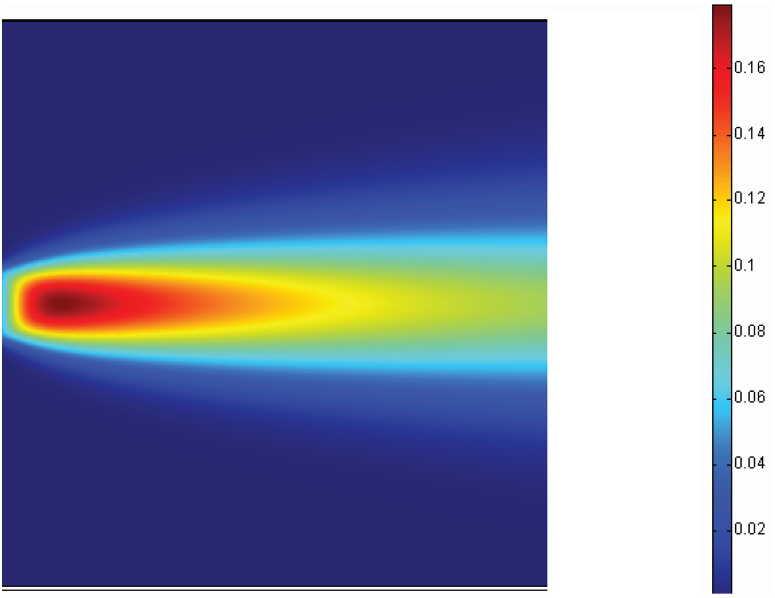

Figure 10. Predicted methane oxidation rate in a horizontal domain 60 km by 60 km (day^{-1}).

of the plume flow rate in the axisymmetric model, with a smaller (half) value to better fit specific oxidation rate data, is consistent with the possibility that tectonic activity in 1999 changed some hydrothermal vent characteristics and increased fluid output (Johnson *et al.*, 2000).

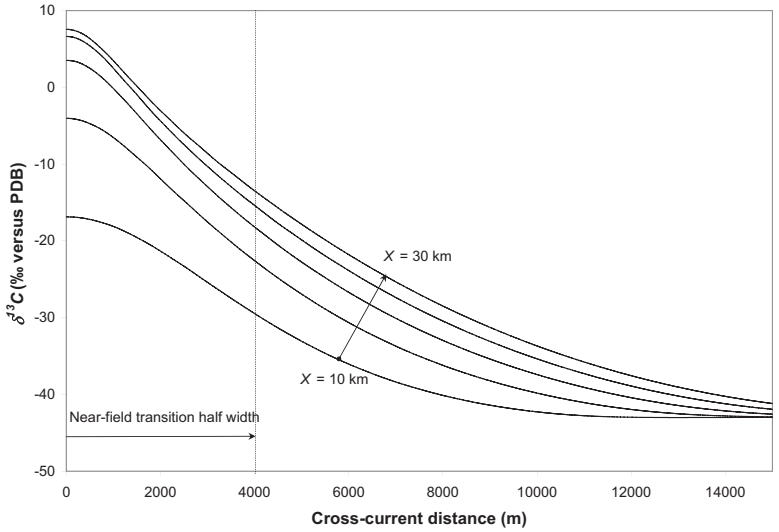

Figure 11. Cross-current half profiles of predicted isotopic composition (two-dimensional model).

Acknowledgements. Funding for this study was provided by the Office of Naval Research through the Hawaii Energy and Environmental Technology Initiative.

APPENDIX A

Vertical mixing above a steady circular hydrothermal vent

The mixing boundary-layer model of Epstein and Burelbach (2001) describes the upward injection of buoyant fluid at a velocity v_0 over a circular area of radius R_0 into another fluid of constant properties (subscript ∞). In the process, ambient fluid is drawn radially inward until conditions for the existence of a rising plume are met, at $r = r_p$. Model assumptions and analytical procedures are not discussed here unless they are of special relevance. Additional details can be found in the reference. In the original analysis, relative buoyancy is generated by releasing freshwater into brine. A hot source into a cold environment would achieve the same result, and these cases can be made undistinguishable by non-dimensionalizing all variables. The Boussinesq approximation is retained even though large density variations may occur in the vicinity of hydrothermal vents (cf. Fig. 1).

The radial distance and boundary-layer thickness are non-dimensionalized with R_0 and noted η and δ^*, respectively. The non-dimensional average inward radial velocity $\bar{u}^*$ and volume flux Q^* are referred to v_0 and $\pi R_0^2 v_0$, respectively. The average buoyancy agent $\bar{\theta}$ is replaced by the non-dimensional variable $\sigma = (\bar{\theta} - \theta_\infty)/(\theta_0 - \theta_\infty)$. A densimetric Froude number is defined for this problem as $F = v_0\{gR_0(\rho_\infty - \rho_0)/\rho_{ref}\}^{-1/2}$. The linear relationship between density and the buoyancy agent (salinity, temperature), is replaced here with the simple quadratic form $\rho \approx \rho_\infty(1 - a_2\theta^2)$. This approach allows density to remain within 5% of exact values over a wide high-temperature range, as shown in Figure 1 with $a_2 = 3.37 \times 10^{-3}\ ^\circ C^{-2}$. Another assumption is that $\theta_\infty = 0^\circ C$. At this point, the derivation in Epstein and Burelbach (2001) can be followed step by step. The integral form of heat conservation is unchanged and Eq. (19) in Epstein and Burelbach (2001) holds. Hydrostatic pressure is affected, however, by the different functional dependence of density on temperature. Subsequent integration of the horizontal momentum equation yields $\bar{u}^* = (0.3\delta^*)^{1/2}\sigma/F$ in lieu of Eq. (18) in Epstein and Burelbach (2001). As a result, the following surface boundary condition is obtained:

$$6^2\beta^2\sigma^2\delta^{*1/2} + 3F\sigma = F \tag{A1}$$

where β is the mixing-length thickness coefficient. Eq. (A1) can further be expressed in terms of only one unknown (e.g. σ) after appropriate substitutions, but an implicit equation is obtained. In the practical low-Froude-number limit, where the convective term $3F\sigma$ is neglected in Eq. (A1), the following explicit solution can be obtained:

$$\begin{cases} \delta^* = 6^2\beta^2\left(\frac{5}{6}\right)^{1/2}\left(\frac{1-\eta^2}{\eta}\right) & \text{(A2)} \\ \bar{u}^* = \frac{1}{25^{3/8}6^{1/8}\beta^{1/2}F^{1/2}}\left(\frac{1-\eta^2}{\eta}\right)^{1/4} & (A3) \\ \sigma = \frac{F^{1/2}}{6^{3/2}\beta^{3/2}}\left(\frac{6}{5}\right)^{1/8}\left(\frac{1-\eta^2}{\eta}\right)^{-1/4} & (A4) \\ Q^* = \frac{6^{3/2}\beta^{3/2}}{F^{1/2}}\left(\frac{5}{6}\right)^{1/8}\eta\left(\frac{1-\eta^2}{\eta}\right)^{5/4} \end{cases} \quad \text{(A5)}$$

An important identity is $Q^*\sigma + \eta^2 = 1$. As in Epstein and Burelbach (2001), the apparent singularity of σ at $\eta = 1$ is the result of discarding the convective term in Eq. (A1); the correct value should be $\sigma(1) = 1/3$ (surface temperature of θ_0 at the edge of the source area).

Next, the transition between mixing boundary layer and buoyant plume is considered. Instead of $Q_p^* \approx Q^*(\eta_p)$ and $\sigma_p \approx \sigma\ (\eta_p)$, i.e. Eq. (25) in Epstein and Burelbach (2001), exact heat and mass balances yield $Q_p^* = Q^*(\eta_p) + \eta_p{}^2$ and $\sigma_p = \{Q^*(\eta_p) + \eta_p{}^2\}^{-1}$. Inserting these values into Eq. (43) in Epstein and Burelbach (2001), the following low-Froude-number equation for η_p is obtained:

$$46^6\left(\frac{5}{6}\right)^{1/2}E\beta^6(1-\eta^2)^5 = \eta^6. \quad \text{(A6)}$$

With β and E about 0.14 and 0.12, respectively, we find that η_p is about 0.55 instead of 0.43 with linear density.

The estimation of vent characteristics from plume initial values $Q(0) = Q_0Q_p^*$ and $\theta(0) = \theta_0\sigma_p$, identified here with transition values from mixing layer to plume per se, could theoretically be done. Since $Q_p^*\sigma_p = 1$, Q_0 can be obtained as $Q(0)\theta(0)/\theta_0$. The knowledge of Q_p^* with Eq. (A5) then yields F (which should be small). Expressing the definitions of Q_0 and F, the radius R_0 and velocity v_0 can be determined straightforwardly.

APPENDIX B

Notations

a	thermal expansion coefficient of seawater ($°C^{-1}$)
a_2	quadratic thermal expansion coefficient of seawater ($°C^{-2}$)
b	buoyant plume radius (m)
c_p	specific enthalpy of seawater ($J\text{-}kg^{-1}\text{-}K^{-1}$)
B	plume buoyancy flux ($m^4\text{-}s^{-3}$)
D	thickness of plume intrusion layer (m)
E	buoyant plume entrainment coefficient
F	densimetric Froude number

g acceleration of gravity (m-s^{-2})
h neutral-buoyancy height of near-field plume above seafloor (m)
H plume heat flux (W)
k methane oxidation rate constant (nM^{-1}-s^{-1})
K far-field eddy diffusion coefficient (m^2-s^{-1})
n number of near-field point sources of buoyancy
N buoyancy frequency (s^{-1})
P eddy diffusion velocity (m-s^{-1})
Q plume volume flux (m^3-s^{-1})
Q_f volume flux in lateral (far-field) plume (m^3-s^{-1})
Q^* non-dimensional radial inward volume flux in mixing boundary layer
r horizontal radial distance from vent field (m)
r_f characteristic length for axisymmetric advection-diffusion processes (m)
R_0 radius of seafloor source of buoyant fluid (m)
R_{PDB} isotopic ratio of PDB standard
s salinity (ppt)
Sp specific methane oxidation rate (s^{-1})
Spm methanotroph biomass-specific oxidation rate (s^{-1})
$\vec{u}$ velocity vector (m-s^{-1})
U current magnitude (m-s^{-1})
$\bar{u}^*$ non-dimensional average radial inward velocity in mixing boundary layer
v_0 upward velocity of vent fluid (m)
x methane concentration (nM)
X horizontal coordinate along current direction (m)
Y horizontal coordinate perpendicular to current direction (m)
y carbon-13 ($^{13}CH_4$) methane concentration (nM)
z methanotroph carbon concentration (nM)
Z vertical coordinate (m)

Greek letters

α carbon assimilation ratio for methanotrophs
β mixing-length thickness coefficient
α_k isotopic fractionation for microbial methane oxidation
δ^* non-dimensional mixing-boundary-layer thickness
$\delta^{13}C$ isotopic composition of methane (‰)
$\delta\rho$ plume density anomaly (kg-m^{-3})
$\delta\theta$ plume temperature anomaly (kg-m^{-3})
η non-dimensional radial coordinate
ρ seawater density (kg-m^{-3})
ρ_{ref} reference density (kg-m^{-3})
σ non-dimensional average temperature across the mixing boundary layer

σ_2 potential density referred to 2000 dbar (kg-m^{-3})

θ temperature (°C)

$\bar{\theta}$ average temperature across the mixing boundary layer (°C)

Subscript

a ambient seawater (plume model with stratification)

p properties at transition from mixing boundary layer to buoyant plume

0 vent fluid (in near-field analysis) or far-field origin

∞ ambient seawater (mixing-layer model with constant properties)

REFERENCES

Bemis, K. G., P. A. Rona, D. Jackson, C. Jones, D. Silver and K. Mitsuzawa. 2002. A comparison of black smoker hydrothermal plume behavior at Monolith Vent and at Clam Acres Vent Field: Dependence on source configuration. Marine Geophys. Res., *23*, 81-96.

Bowman, J. P., S. A. McCammon and J. H. Skerratt. 1997. *Methylosphaera hansonii* gen. nov., sp. nov., a psychrophilic, group I methanotroph from Antarctic marine-salinity, meromitic lakes. Microbiol., *143*, 1451-1459.

Button, D. K. and B. Robertson. 1999. Properties of small free-living aquatic bacteria, *in* Size Limits of Very Small Microorganisms – Proceedings of a Workshop, The National Academies Press, 164 pp.

Cowen, J. P., X. Wen and B. N. Popp. 2002. Methane in aging hydrothermal plumes. Geochim. Cosmochim. Acta, *66*, 3563-3571.

Craig, H. 1957. Isotopic standards for carbon and oxygen and correction factors for mass spectrometric analysis of carbon dioxide. Geochim. Cosmochim. Acta, *12*, 133-149.

de Angelis, M. A., J. A. Baross and M. D. Lilley. 1991. Enhanced microbial methane oxidation in water from a deep-sea hydrothermal vent field at simulated *in situ* hydrostatic pressures. Limnol. Oceanogr., *36*, 565-570.

de Angelis, M. A., M. D. Lilley. E. J. Olson and J. A. Baross. 1993. Methane oxidation in deep-sea hydrothermal plumes of the Endeavour Segment of the Juan de Fuca Ridge. Deep-Sea Res., *40*, 1169-1186.

DeLong, E. F. 1999. Diminutive cells in the ocean – Unanswered questions, *in* Size Limits of Very Small Microorganisms – Proceedings of a Workshop, The National Academies Press, 164 pp.

Epstein, M. and J. P. Burelbach. 2001. Vertical mixing above a steady circular source of buoyancy. Int. J. Heat Mass Trans., *44*, 525-536.

Fofonoff, N. P. and R. C. Millard Jr. 1983. Algorithms for computation of fundamental properties of seawater. UNESCO Tech. Papers in Mar. Sci., *44*, 53 pp.

Fukuda, R., H. Ogawa, T. Nagata and I. Koike. 1998. Direct determination of carbon and nitrogen contents of natural bacterial assemblages in marine environments. Appl. Environ. Microbiol., *64*, 3352-3358.

Grant, N. J. and M. J. Whiticar. 2002. Stable carbon isotopic evidence for methane oxidation in plumes above Hydrate Ridge, Cascadia Oregon Margin. Global Biogeochem. Cy., *16*, 13 pp.

Harrits, S. M. and R. S. Hanson. 1980. Stratification of aerobic methane-oxidizing organisms in Lake Mendota, Madison, Wisconsin. Limnol. Oceanogr., *25*, 412-421.

Hewett, T. A., J. A. Fay and D. P. Hoult. 1971. Laboratory experiments of smokestack plumes in a stable atmosphere. Atm. Env., *5*, 767-789.

Huang, H., R. E. Fergen, J. R. Proni and J. J. Tsai. 1998. Initial dilution equations for buoyancy-dominated jets in current. ASCE J. Hydr. Eng., *124*, 105-108.

Hutton, W. E. and C. E. Zobell. 1949. The occurrence and characteristics of methane-oxidizing bacteria in marine sediments. J. Bact., *58*, 463-473.

Johnson, H. P., M. Hutnak, R. P. Dziak, C. G. Fox, I. Urcuyo, J. P. Cowen, J. Nabelek and C. Fisher. 2000. Earthquake-induced changes in a hydrothermal system on the Juan de Fuca mid-ocean ridge. Nature, *407*, 174-177.

Jones, R. D., R. Y. Morita and R. P. Griffiths. 1984. Method for estimating *in situ* chemolithotrophic ammonium oxidation using carbon monoxide oxidation. Mar. Ecol. Prog. Ser., *17*, 259-269.

Joseph, J. and H. Sendner. 1958. The horizontal diffusion in the ocean. Deutsche Hydrographische Zeitschrift*, 11*, 49-77.

Lupton, J. E., J. R. Delaney, H. P. Johnson and M. K. Tivey. 1985. Entrainment and vertical transport of deep-ocean water by buoyant hydrothermal plumes. Nature, *316*, 621-623.

Morton, B. R., G. I. Taylor and J. S. Turner. 1956. Turbulent gravitational convection from maintained and instantaneous sources. Proc. Royal Soc. Lond.., *A234*, 1-23.

National Institute of Standards and Technology. 2005. Thermophysical Properties of Fluid Systems. U. S. Dept. of Commerce online data base, http://webbook.nist.gov/chemistry/fluid/

Nihous, G. C. 2006. Near-field evaluation of artificial upwelling concepts for open-ocean oligotrophic conditions. J. Mar. Env. Eng., *8*, 225-246.

——2007. Far-field evaluation of a Lagrangian artificial upwelling concept. J. Mar. Env. Eng., *9*, 17-35.

Nihous, G. C. and S. M. Masutani. 2006. A model of methane concentration profiles in the open ocean. J. Mar. Res., *64*, 629-650.

Reeburgh, W. S. 2007. Oceanic methane biogeochemistry. Chem. Rev., *107*, 486-513.

Rehder, G., R. S. Keir and E. Suess. 1999. Methane in the Northern Atlantic controlled by microbial oxidation and atmospheric history. Geophys. Res. Lett., *26*, 587-590.

Roberts, P. J. W., W. H. Snyder and D. J. Baumgartner.1989. Ocean outfalls: I: Submerged wastefield formation. II: Spatial evolution of submerged wastefield. III: Effect of diffuser design on submerged wastefield. J. Hydr. Eng., *115*, 1-70.

Rona, P. A., K. G. Bemis, D. Silver and C. D. Jones. 2002. Acoustic imaging, visualization, and quantification of buoyant hydrothermal plumes in the ocean. Marine Geophys. Res., *23*, 147-168.

Scranton, M. I. and P. G. Brewer. 1978. Consumption of dissolved methane in the deep ocean. Limnol. Oceanogr., *23*, 1207-1213.

Screening Information Data Sets of the Organisation for Economic Co-operation and Development (OECD SIDS). 2000. Example of Diacetone Alcohol, Case 123-42-2. UNEP Pub., http://www.chem.unep.ch/irptc/sids/OECDSIDS/123422.pdf, 138-165.

Sieburth, J. McN., P. W. Johnson, V. N. Church and D. C. Laux. 1993. C_1 bacteria in the water column of Chesapeake Bay, USA. III. Immunologic relationships of the type species of marine monomethylamine- and methane-oxidizing bacteria to wild estuarine and oceanic cultures. Mar. Ecol. Prog. Ser., *95*, 91-102.

Sieburth, J. McN., P. W. Johnson, M. A. Eberhardt, M. E. Sieracki, M. Lidstrom and D. C. Laux. 1987. The first methane-oxidizing bacterium from the upper mixing layer of the deep ocean: *Methylomonas pelagica* sp. nov. Current Microbiol., *14*, 285-293.

Steele, J. H. and E. W. Henderson. 1992. The role of predation in plankton models. J. Plankton Res., *14*, 157-172.

Sundh, I., D. Bastviken and L. J. Tranvik. 2005. Abundance, activity, and community structure of pelagic methane-oxidizing bacteria in temperate lakes. Appl. Environ. Microbiol., *71*, 6746-6752.

Valentine, D. L., D. C. Blanton, W S. Reeburgh and M. Kastner. 2001. Water column methane

oxidation adjacent to an area of active hydrate dissociation, Eel River Basin. Geochim. Cosmochim. Acta, *65*, 2633-2640.

Ward, B. B. 1987. Kinetic studies on ammonia and methane oxidation by *Nitrosococcus oceanus*. Arch. Microbiol., *147*, 126-133.

Ward, B. B. and K. A. Kilpatrick.1993. Methane oxidation associated with mid-depth methane maxima in the Southern California Bight. Cont. Shelf Res., *13*, 1111-1122.

Weast, R. C., ed. 1975. Mathematical Tables *in* Handbook of Chemistry and Physics, 56th edition. CRC Press, A1-A192.

Whittenbury, R., K. C. Phillips and J. F. Wilkinson. 1970. Enrichment, isolation and some properties of methane-utilizing bacteria. J. General Microbiol., *61*, 205-216.

Wright, S. J. 1977. Mean behavior of buoyant jets in a crossflow. ASCE J. Hydr. Div., *103*, 499-513.

Wright, S. J., D. R. Wong, K. E. Zimmerman and R. B. Wallace. 1982. Outfall diffuser behavior in stratified ambient fluid. ASCE J. Hydr. Div., *108*, 483-501.

Received: *29 June, 2007*; revised : *7 November, 2007*.